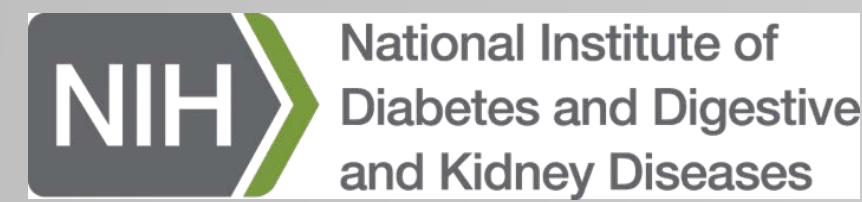


# Understanding hepatitis delta virus and HBsAg kinetics during treatment with prenylation inhibitor lonafarnib via mathematical modeling

Laetitia Canini<sup>1,2</sup>, Christopher Koh<sup>3</sup>, Scott J. Cotler<sup>1</sup>, Xiongce Zhao<sup>4</sup>, Susan L. Uprichard<sup>1</sup>, Vanessa Haynes-Williams<sup>3</sup>, Mark A. Winters<sup>5</sup>, Gitanjali Subramanya<sup>1</sup>, Stewart Cooper<sup>6</sup>, Peter Pinto<sup>7</sup>, Erin Wolff<sup>8</sup>, Rachel Bishop<sup>9</sup>, Ma Ai Thanda Han<sup>3</sup>, David E. Kleiner<sup>10</sup>, Onur Keskin<sup>11</sup>, Ramazan Idilman<sup>11</sup>, Cihan Yurdaydin<sup>11</sup>, Jeffrey S. Glenn<sup>5</sup>, Theo Heller<sup>3\*</sup> and Harel Dahari<sup>1,12\*</sup>

The Program for Experimental & Theoretical Modeling, Division of Hepatology, Loyola University Medical Center, Maywood, Illinois<sup>1</sup>; Centre for Immunity, Infection and Evolution, University of Edinburgh, Edinburgh, United Kingdom<sup>2</sup>; Translational Hepatology Unit, Liver Diseases Branch, National Institute of Diabetes & Digestive & Kidney Diseases, National Institutes of Health, Bethesda, Maryland<sup>3</sup>; Office of the Director, National Institute of Diabetes & Digestive & Kidney Diseases, National Institutes of Health, Bethesda, Maryland<sup>4</sup>; Departments of Medicine (Division of Gastroenterology and Hepatology) and Microbiology & Immunology, Stanford School of Medicine, Stanford, California<sup>5</sup>; Division of Hepatology, California Pacific Medical Center, San Francisco, California<sup>6</sup>; Urologic Oncology Branch, National Cancer Institute, National Institutes of Health, Bethesda, Maryland<sup>7</sup>; Unit on Reproductive and Regenerative Medicine, National Institute of Child Health and Human Development<sup>8</sup>; Consult Services Section, National Eye Institute, National Institutes of Health, Bethesda, Maryland<sup>9</sup>; Laboratory of Pathology, National Cancer Institute, National Institutes of Health, Bethesda, Maryland<sup>10</sup>; Department of Gastroenterology, Ankara University, Ankara, Turkey<sup>11</sup>; Theoretical Biology & Biophysics Group, Los Alamos National Laboratory, Los Alamos, New Mexico<sup>12</sup>. \*These authors share senior authorship



## 1. Background & Aims

15-20 million people are infected worldwide with chronic hepatitis D (HDV). Up to 80% of patients with HDV may develop cirrhosis within 5-10 years. Interferon-based therapy is unsatisfactory, <30% achieve HBsAg loss and become HDV RNA negative. Nucleos(t)ide analogues are ineffective. Prenylation inhibition has demonstrated effectiveness against HDV in vitro & in vivo models [1-6]. The prenylation inhibitor lonafarnib (LNF) is a potent antiviral agent that provides a breakthrough for the treatment of HDV and an opportunity to further characterize HDV and hepatitis B surface antigen (HBsAg) dynamics during effective treatment with an oral anti-HDV agent.

## 2. Patients, Study Design & Kinetic Data

14 chronically infected HDV patients were sequentially enrolled into 2 groups in a phase 2a double-blinded, randomized, placebo-controlled study (Fig. 1 and Table 1). Patients received treatment for 28 days, followed by post-treatment monitoring for six months.

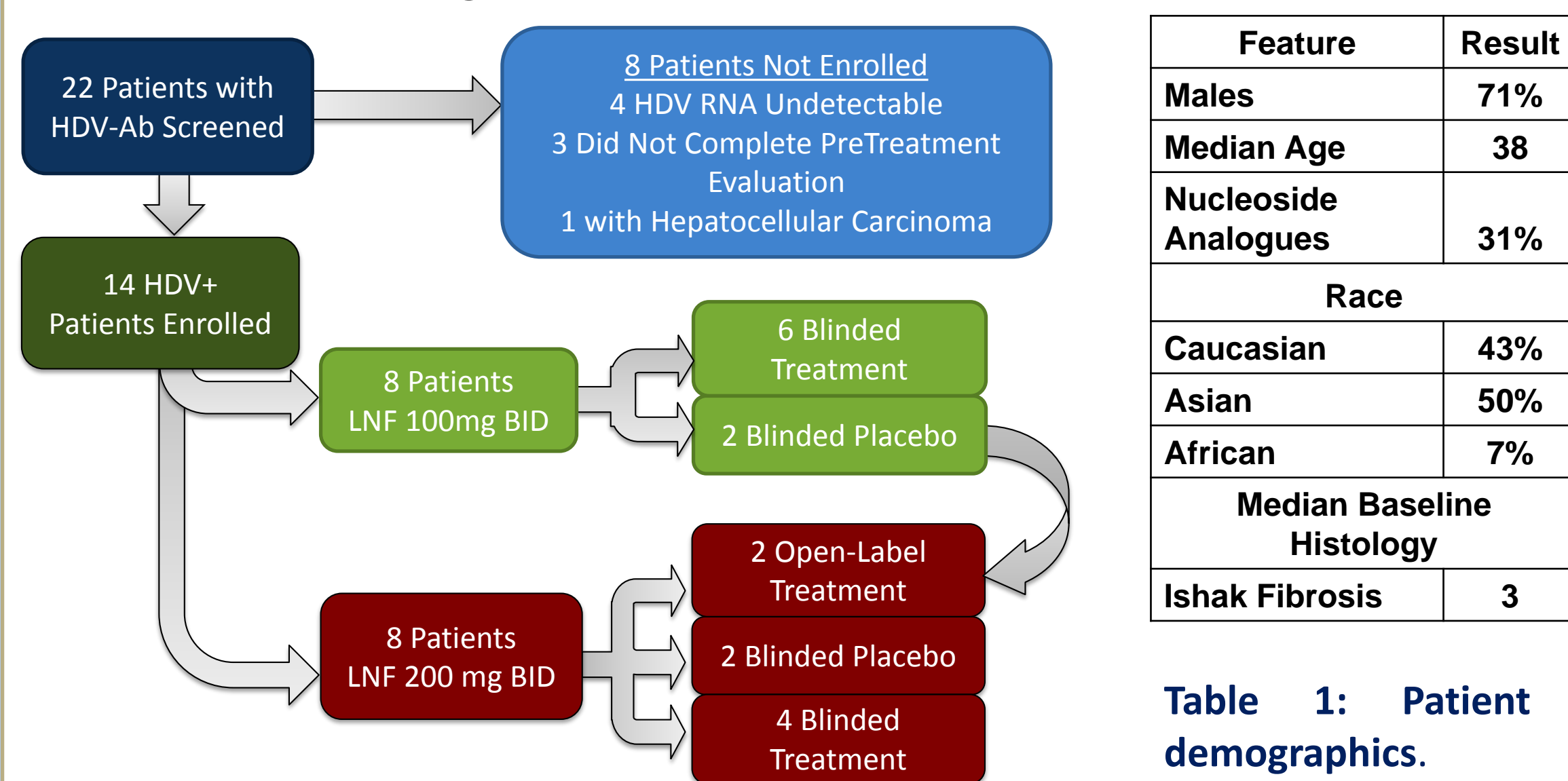


Figure 1: Study Flow.

Blood samples were collected frequently during the first 72 hr, and then weekly until day 28. Quantitative HBV DNA levels were measured by qPCR. Quantitative HBsAg (qHBsAg) levels were measured on stored serum samples using the International Immuno-Diagnostics enzyme-linked immune assay (ELISA) with HBsAg standards from Alpha Diagnostics International.

## 3. Dual Model Description

The kinetics of HDV and HBsAg during LNF therapy was modeled using our dual model (Fig. 2) for HDV and HBsAg kinetics during pegIFN therapy [7].

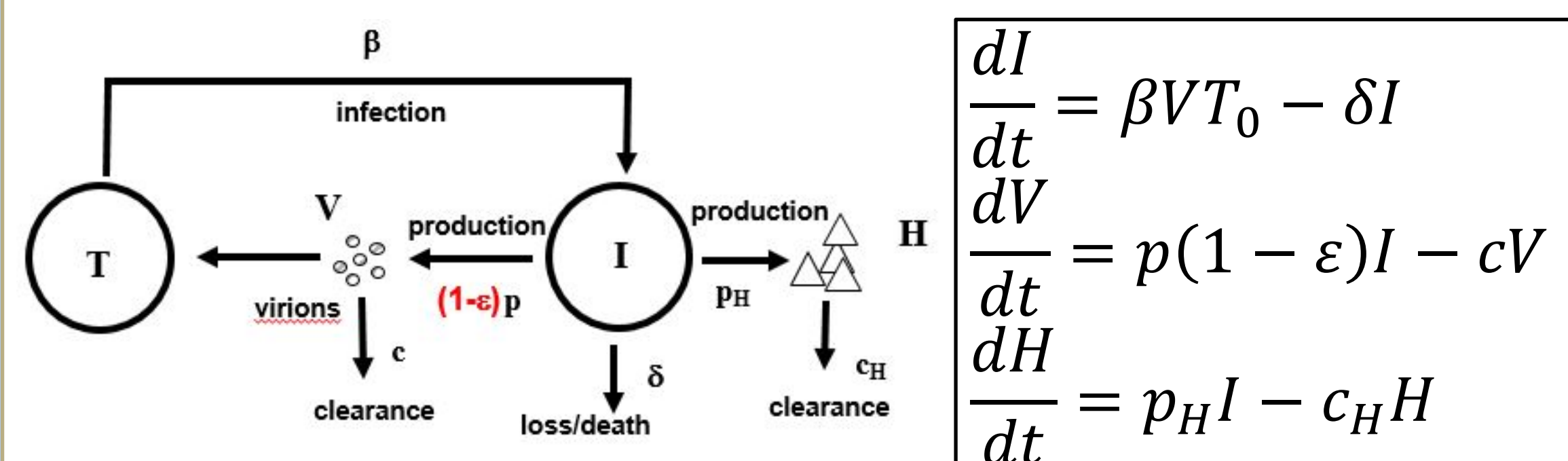


Figure 2. Dual Model Schematic.

$I$ : HBsAg-infected cells that can produce HDV virion;  $V$ : HDV RNA level in blood;  $H$ : serum HBsAg level.  $\beta$ : infectivity rate;  $p$ : HDV production rate,  $\delta$ : infected cell loss rate;  $c$ : HDV clearance rate;  $\epsilon$ : LNF effectiveness;  $p_H$ : HBsAg production rate;  $c_H$ : HBsAg clearance rate.

We assume the target cell i.e., HBsAg-productive cell, count was constant during 28 days with lonafarnib treatment and equal to its pre-treatment steady-state value  $T_0 = c\delta/\beta p$ .

Assuming that HDV and HBsAg are in equilibrium before treatment initiation, the model can be simplified such that  $p_H = \frac{p \times H_0}{c \times V_0}$ , where  $H_0$  and  $V_0$  are the initial levels of serum HBsAg and HDV, respectively.

**Model simulations and sensitivity analysis:** We simultaneously fitted the model to the log-scaled HDV viral loads and HBsAg levels, using a nonlinear mixed effect modeling approach. Population estimates and inter-individual variability (IIV) estimates were obtained using a maximum-likelihood method implemented in MONOLIX version 4.3.2.

## 4. HDV RNA & HBsAg Kinetics

- HBsAg remains at baseline levels (Fig. 3)
- Biphasic decline during therapy in all LNF-treated patients (Fig. 3)
- First rapid decline phase followed by a second slower (or plateau) phase (Table 2).
- First phase duration longer in Group 2 compared to Group 1 (Table 2). Faster decline in Group 2, leading to a significantly greater 1st-phase decline in Group 2 than in Group 1 (1.59 vs. 0.78 log IU/mL,  $p=0.015$ )
- The second slope phase was not statistically different between Groups 2 and 1 (Table 2).

Lonafarnib treatment	Baseline HDV RNA [log IU/mL] (se)	1 <sup>st</sup> phase slope [log IU/mL/d] (se)	2 <sup>nd</sup> phase slope [log IU/mL/d] (se)	Transition time [d] (se)
100 mg bid	8.01 (0.06)	-0.098 (0.03)	-0.04 (0.04)	8.72 (2.5)
200 mg bid	7.80 (0.07)	-0.143 (0.02)	0.004 (0.03)	12.3 (2.1)
P-value	0.70	0.07	0.94	0.31

**Table 2: HDV 1st and 2nd phase slopes and their transition time by segmented linear regression (SLR).** To predict the transition time between the 1<sup>st</sup> and 2<sup>nd</sup> phases and to estimate their slopes we used the segmented linear regression package called 'segmented 0.5-0.0' in R 3.1.1. Parameter fitting was performed by maximum-likelihood method, using the log-scaled viral loads. If the second slope was significantly different from the first slope, we considered the patients exhibited a biphasic viral load decline. se stands for standard error

## References

- Hughes SA, et al. Lancet 2011;378
- Colombo M, et al. Gastroenterol 1983;85
- Manesis EK, et al. J Hep 2013;59
- Wedemeyer H, et al. Hepatology 2013; 58
- Heller T, et al. Aliment Pharmacol Ther 2014; 40
- Bordier BB, et al. J Clin Invest 2003;112
- Guedj et al. Hepatology 2014; 60:1902-1910
- Guedj/Dahari PNAS;2013;110:3991-6

## Conclusions

- ❑ The observed stable HBsAg level during LNF treatment suggests that the productively HDV-infected cell number remained unchanged during this relatively short treatment period.
- ❑ The modeling analysis indicated a dose dependent effect of LNF in blocking HDV release with efficacies of 74% and 95% in the Groups 1 and 2, respectively. Moreover, the 95% efficacy of the 200 mg LNF dose was similar to recent estimates in patients treated with peg-IFN [7] ( $\epsilon=96\%$ ) and was achieved much earlier with LNF (median 12.5 days) compared to pegIFN (median 25.2 days).
- ❑ A strikingly shorter delay was observed with LNF ( $t_0=0.73$  day) compared to HDV-infected patients treated with peg-IFN ( $t_0=8.5$  day).
- ❑ Frequent measurements under LNF therapy allowed for a refined estimate of HDV  $t_{1/2}=1.6$  day that was about 2-fold shorter than under peg-IFN ( $t_{1/2}=2.9$  day), and suggests a higher HDV production rate than recently estimated [7].
- ❑ This shorter  $t_{1/2}$  is reminiscent of the dual mechanism of action observed with an HCV NS5A inhibitor [8], which suggests that LNF might similarly have two mechanisms of action that result from inhibiting farnesylation of large delta antigen: one involving inhibition of HDV particle production, and a second resulting from increased retention of intracellular unprenylated LDHAg, which in turn can increase LDHAg's transdominant inhibitory effect on HDV RNA genome replication.
- ❑ Additional viral kinetic analyses based on these results and future studies should help enable determination of the optimal dose and duration needed to ensure proper eradication of those infected with HDV.

## 5. Model Fits & Parameter Estimations

- Fitting the HDV and HBsAg dual model (Fig. 3) with measured HDV and HBsAg kinetics yielded excellent fit curves.
- The pretreatment serum HDV RNA and HBsAg levels were estimated as 5.97(se=0.13) log IU/mL and 4.17(se=0.12) log ng/mL.
- A short pharmacological delay of  $t_0=0.73$  (se=0.24) day, in which HDV remained at baseline levels, was not associated with LNF dose.
- The HDV clearance rate in blood,  $c$ , was estimated as 0.426 (se=0.04) d<sup>-1</sup>, corresponding to an HDV half-life in blood of 1.63 (se=0.15) days.
- LNF effectiveness in blocking HDV production was significantly ( $p<0.001$ ) higher in Group 2 ( $\epsilon=0.952$  (se=0.057)) than Group 1 ( $\epsilon=0.739$  (se=0.05))

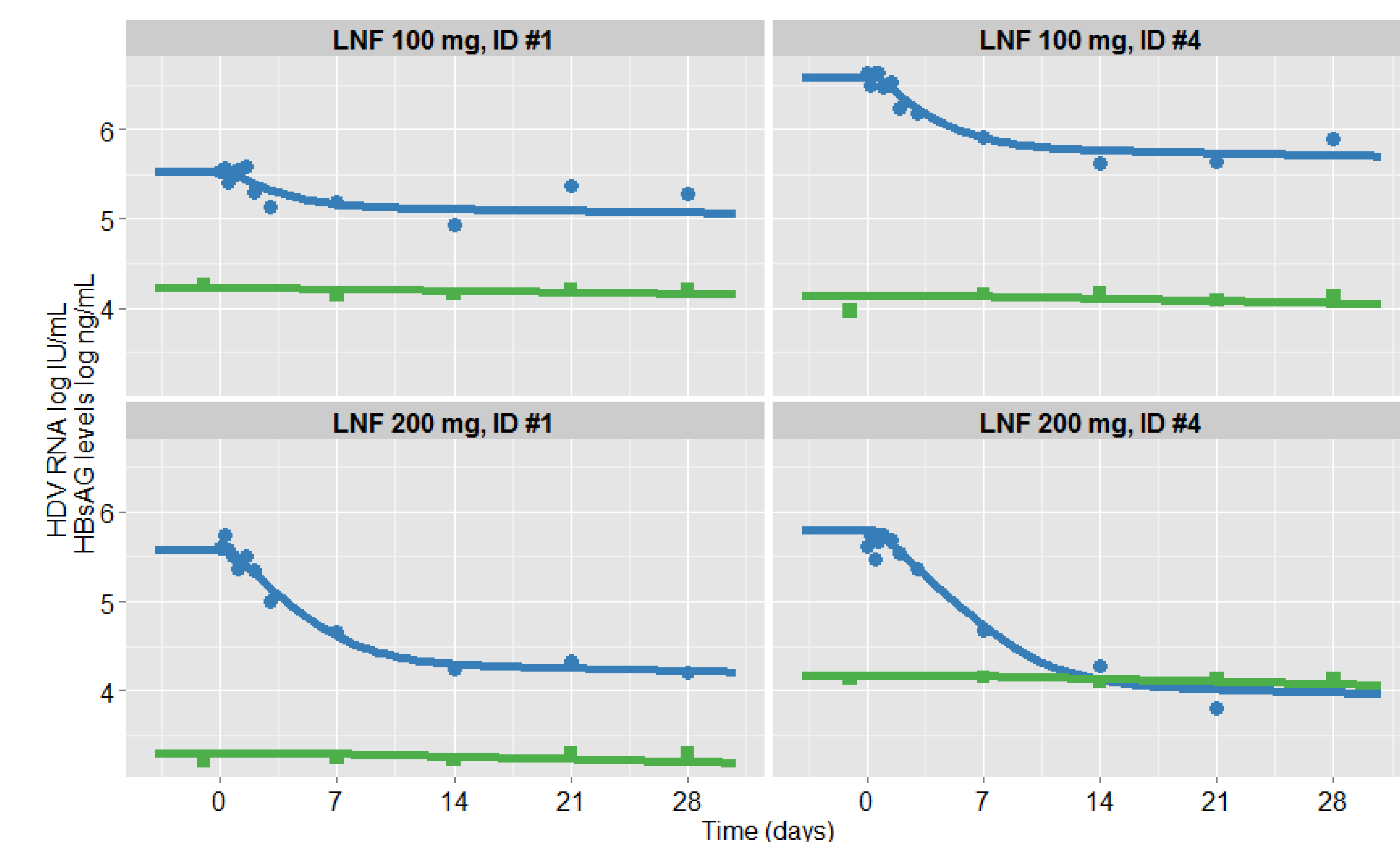


Figure 3: HDV and HBsAg kinetics and modeling during 100 (Upper panels) or 200 (Lower panels) mg bid of lonafarnib (LNF). HDV viral load and HBsAg levels observations are shown with blue circles and green squares, respectively. The best-fit curves are shown in blue and green for HDV viral load and HBsAg levels, respectively.

Parameter [unit]	Parameter description	Population value (se)	Inter-individual variability % (se)
$t_0$ [d]	Pharmacological delay	0.73 (0.24)	66 (33)
$\ln(2)/c$ [d]	HDV half-life in blood	1.63 (0.07)	16 (11)
$\epsilon^*$	Group 1	0.739 (0.05)	15 (3)
	Group 2	0.952 (0.057)	
$V_0$ [log <sub>10</sub> IU/mL]	Pre-treatment HDV viral load	5.97 (0.13)	7.5 (1.6)
$H_0$ [log <sub>10</sub> ng/mL]	Pre-treatment HBsAg level	4.17 (0.12)	9.5 (2.0)

The death/loss rate of productively HDV-infected cell was fixed to  $\delta=0.01$  to account for the observed kinetics of both HDV and HBsAg. \*,  $\epsilon$  is significantly ( $p=0.0056$ ) higher in Group 2 compared to Group 1.

## Acknowledgements

This work was supported by the intramural research programs of the NIDDK, NCI & NICHD, NIH, and was supported by NIH grant P20-GM103452. Portions of this work were done under the auspices of the U.S. Department of Energy under contract DE-AC52-06NA25396

## Disclosures

Lonafarnib was provided by Eiger Biopharmaceuticals, Inc under a clinical trial agreement (#NCT01495585) with the NIDDK, NIH. Glenn: Equity interest in Eiger Biopharmaceuticals, Inc. Dahari: Received partial travel support from Eiger Biopharmaceuticals, Inc to attend scientific meetings. All other authors have no financial disclosures.